Effects of Cryopreservation on the Depth-Dependent Elastic Modulus in Articular Cartilage and Implications for Osteochondral Grafting

David Kahn
Department of Physics and Center for Biomedical Research,
Oakland University,
2200 N Squirrel Road,
Rochester, MI 48309
e-mail: djkahn@oakland.edu

Clifford Les
Department of Physics,
Oakland University,
2200 N Squirrel Road,
Rochester, MI 48309
e-mail: les@oakland.edu

Yang Xia
Department of Physics and Center for Biomedical Research,
Oakland University,
2200 N Squirrel Road,
Rochester, MI 48309
e-mail: xia@oakland.edu

Cryopreservation of articular cartilage is often used in storage of experimental samples and osteochondral grafts, but the depth-dependence and concentration of glycosaminoglycan (GAG) are significantly altered when cryogenically stored without a cryoprotectant, which will reduce cartilage stiffness and affect osteochondral graft function and long-term viability. This study investigates our ability to detect changes due to cryopreservation in the depth-dependent elastic modulus of osteochondral samples. Using a direct-visualization method requiring minimal histological alterations, unconfined stepwise stress relaxation tests were performed on four fresh (never frozen) and three cryopreserved (−20 °C) canine humeral head osteochondral slices 125 ± 5 μm thick. Applied force was measured and tissue images were taken at the end of each relaxation phase using a 4× objective. Intratissue displacements were calculated by tracking chondrocytes through consecutive images for various intratissue depths. The depth-dependent elastic modulus was compared between fresh and cryopreserved tissue for same-depth ranges using analysis of variance (ANOVA) with Tukey post-test with a 95% confidence interval. Cryopreservation was found to significantly alter the force–displacement profile and reduce the depth-dependent modulus of articular cartilage. Excessive collagen fiber folding occurred at 40–60% relative depth, producing a "black line" in cryopreserved tissue. Force–displacement curves exhibited elongated toe-region in cryopreserved tissue while fresh tissue had nonmeasurable toe-region. Statistical analysis showed significant reduction in the elastic modulus and GAG concentration throughout the tissue between same-depth ranges. This method of cryopreservation significantly reduces the depth-dependent modulus of canine humeral osteochondral samples. [DOI: 10.1115/1.4029182]

Manuscript received August 22, 2014; final manuscript received November 10, 2014; published online March 6, 2015. Assoc. Editor: Ram Devireddy.

Introduction

Articular cartilage is the load bearing, low friction tissue covering the ends of bones in synovial joints and can withstand great forces by distributing stress through compressive displacement [1,2]. This highly complex tissue is composed mainly of water, collagen fibers, and proteoglycans made of negatively charged GAG molecules attached to a protein core. The collagen fibers in articular cartilage are anisotropically organized into three zones along its thickness in a depth-dependent manner. From the articular surface (AS) to the cartilage–bone interface, or tidemark (TM), the zones include a superficial zone (SZ), transitional zone (TZ), and radial zone (RZ) in which collagen fibers are oriented parallel, randomly, and perpendicular to the AS, respectively. In healthy articular cartilage, molecular properties such as collagen content and GAG concentration increase through tissue depth [3,4] and give rise to increasing depth-dependent elastic modulus [5–8] through hydraulic and osmotic pressure, and electronegative repulsion of GAG molecules [9–11].

Over time, cartilage function can diminish due to disease such as osteoarthritis (OA), which affects most of the adult human population [12,13]. Patients experiencing advanced OA symptoms, such as chronic joint pain and stiffness, but who do not require full joint replacement, may instead select an osteochondral grafting procedure. A major shortcoming for a procedure of this nature is cryopreservation of osteochondral plugs prior to implantation. The depth-dependence and concentration of GAG are significantly altered due to physical or biochemical damage when stored without a cryoprotectant such as dimethyl sulfoxide, a chemical that protects against cryodamage but has high cellular toxicity [4]. Since the static load bearing capability of cartilage is highly dependent on GAG concentration [7], a reduction in GAG concentration could affect osteochondral graft function. Improper load distribution in cryopreserved cartilage may also have effects on chondrocyte survival. For example, Muldrew et al. found 1 yr after transplanting cryopreserved osteochondral grafts, chondrocytes were nonexistent in the intermediate zone (approximately 50% relative tissue depth) [14,15]. Reduced cartilage stiffness may cause overloading of chondrocytes, eventually causing annihilation.

The understanding of intratissue load distribution is of great importance in cryobiology. Techniques used in cartilage repair need to promote long-term health benefits, and an understanding of depth-dependent compressive changes due to cryopreservation of cartilage is vital. By using a technique developed by Szarko and Xia [8], it is possible to visually track intratissue chondrocyte displacement using minimally altered tissue samples to obtain quantitative depth-dependent stiffness measurements. We hypothesize the reduction in depth-dependent GAG concentration will significantly reduce the depth-dependent elastic modulus, an incident that may lead to abnormal cartilage mechanics and decreased osteochondral graft viability. This investigation aims to measure the depth-dependent modulus alteration using one osteochondral cryopreservation method and to verify our ability to detect those changes. Gaining an understanding of cryopreservation effects on the depth-dependent modulus will aid in determining the most effective way to preserve osteochondral grafts.

Materials and Methods

Specimen Preparation. Four shoulder joints were harvested from four healthy mature canines sacrificed for an unrelated experiment. Each joint (scapula, humerus, synovial lining, and muscle) was stored intact at 4 °C and opened within 24 h of harvesting. After opening, seven osteochondral blocks approximately 2.6 × 5 mm were cut from the center region of humeral heads using a low speed diamond saw (MTI Model 150, Richmond, CA).

Of the seven tissue blocks, four were designated as the fresh group and three were designated as the −20 °C group. Fresh osteochondral blocks were stored at 4 °C in a 154 mM saline solution with 1% protease inhibitor (saline-PI) for 3 days or less during experimentation. Cryopreserved tissue blocks were immersed in the same saline-PI solution and frozen at −20 °C for at least 3 days then thawed at 4 °C overnight. Cryopreserved samples were immersed in a 1 mM gadolinium solution (Gd-DTPA^{2-}) for at least 12 h to force fragmented GAG particles from the tissue, then bathed for approximately one day in three separate high-volume saline-PI bath to clear gadolinium (Gd) ions from the tissue. Additional tests were performed using two cryopreserved blocks without the introduction of Gd ions to compare Gd effects on cartilage.

Biomechanical Protocol. From each of the seven blocks, 125 ± 5 μm full-depth osteochondral slices were cut using a Leica VT1000s vibratome (Buffalo Grove, Il). Following vibratomy, the slices were trimmed using a razorblade from 2.6 mm wide to 1–2 mm wide to minimize AS curvature. Biomechanical testing was performed using a homemade apparatus consisting of a Zaber Technologies T-LA28A computer-controlled motorized micrometer and Transducer Techniques 25 g piezoelectric load cell attached to a rigid frame with a fluid chamber and clear glass window. The testing device was affixed to a Nikon Diaphot inverted microscope with an 18 megapixel Canon T4i camera and 4× objective lens that yielded 0.435 μm pixel resolution. Load sensor voltage readings from applied force were measured using a Tenma 72-6900 dual-display multimeter. A calibration loading curve was measured for the sensor to convert voltage to grams.

A representative diagram of the setup is shown in Fig. 1. The 125 μm-thick tissue slice was placed in a homemade glass cassette open along the AS and sides, allowing for only two-dimensional expansion. The bone side pressed against the closed edge. The cassette and fluid chamber were filled with fresh 154 mM saline-PI solution and the cassette was placed against the load sensor. The voltmeter was tared, a compression platen made from a glass cover slide was moved close to the AS, and an image was taken of the uncompressed cartilage. Stepwise unconfined stress relaxation tests were performed using incremental compression steps of approximately 30 μm at a rate of 4.65 μm/s. Final surface strains were 30–35% and adequate relaxation time (typically 5–10 min) was allowed between each subsequent step. At the end of each relaxation phase, the resultant force was recorded and an image was taken.

Image Analysis Protocol. The displacement of chondrocytes at incremental intratissue depths (approximately every

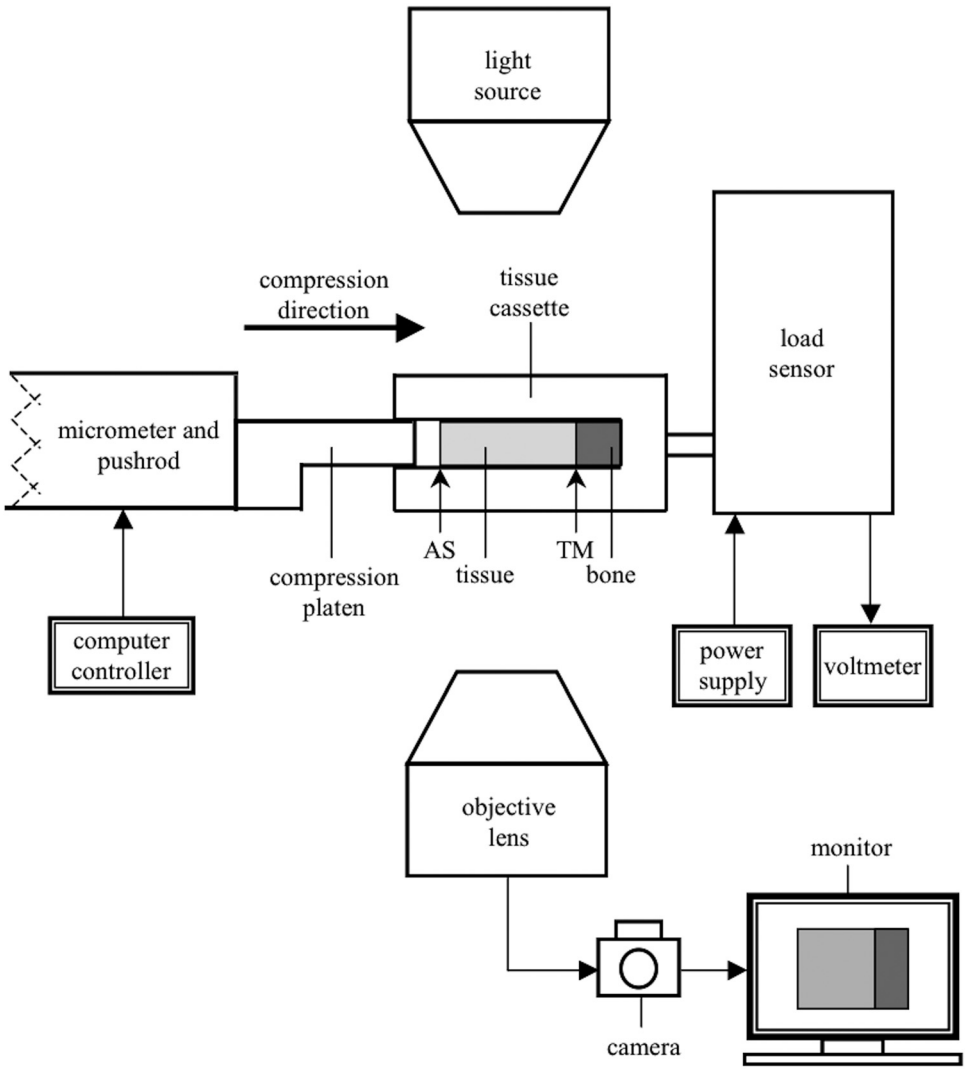

Fig. 1 A representative diagram of the experimental setup (not to scale). Not indicated is the clear glass window (directly below the tissue cassette) or the 154 mM bathing solution (surrounding the tissue). The direction of compression is along the axial direction (horizontal in the figure).

50–100 μm) was tracked throughout consecutive compression images to obtain depth-dependent displacement profiles. For each image, a measurement along the axial direction (direction of compression) was taken from the AS to the TM and a chondrocyte to the TM to calculate "bulk" (whole tissue) and intratissue displacement, respectively. An additional measurement from the uncompressed image was made from the AS to a chondrocyte to measure chondrocyte intratissue depth. These measurements were used in determining bulk and intratissue stiffness. The tissue was modeled as a Hookian material to simplify the comparison between fresh and cryopreserved tissue. Stiffness was calculated by fitting a straight line through the linear portion (typically the last four points) of force–displacement curves for each chondrocyte. The slope of the straight-line fit was used in calculating the elastic modulus at equilibrium.

Statistical Protocol. ANOVA with Tukey post-test with 95% confidence interval was used to determine statistical significance between fresh and cryopreserved tissue for modulus and GAG concentration. Comparisons were made for same-depth ranges of fresh and cryopreserved cartilage; i.e., fresh and cryopreserved values for identical depth ranges (0–10%, 10–20%, etc.) were compared. A p value of <0.05 indicated statistical significance and a p value of <0.001 indicated high statistical significance.

Results

Visual Observations. Figure 2 is a set of representative images that show chondrocyte displacement in different zones for several strains. The circled chondrocytes and connecting arrows qualitatively show the varying intratissue strains for several depths. Compressions appear very similar between fresh (Fig. 2(*a*)) and cryopreserved (Fig. 2(*b*)) cartilage. The upper zones (nearer the AS) have smaller compressive modulus and hence undergo compression prior to deeper zones, which has also been found in other investigations [5,8]. A distinct difference is the formation of a black line (fold) in the cryopreserved tissue that formed between 40% and 60% relative depths (indicated by the thick white arrows). This black line was observed in all Gd-treated cryopreserved specimens, but not in others.

Force–Displacement. Typical force–displacement curves are shown in Fig. 3 at three relative depths for (*a*) fresh tissue and (*b*) cryopreserved tissue. Many changes in tissue properties postfreezing can be seen in these plots. The resultant maximum force of fresh tissue is approximately four times greater than cryopreserved tissue for similar bulk-tissue strains. There is an apparent inverted trend in the force–displacement curves between fresh and cryopreserved tissue. Fresh tissue exhibits greater slope at lesser displacement (concave-down), while the cryopreserved tissue exhibits greater slope at greater displacement (concave-up). In the SZ and upper RZs, the fresh tissue reached linearity at low displacements (10–30 μm), but in direct contrast the cryopreserved tissue reached linearity at much greater displacements. One similarity of fresh and cryopreserved tissue is the nearly identical total displacement for equal intratissue depths.

Modulus and GAG. Figure 4 shows distinct change in the depth-dependent elastic modulus and GAG concentration for (*a*) fresh and (*b*) cryopreserved tissue. The GAG concentrations, determined in a previous study by microscopic magnetic resonance imaging (μMRI) dGEMRIC method [4], were reanalyzed into 10% relative depth increments to compare with the current biomechanical results. (The canine specimens used in both the previous μMRI study and the current study all came from the same tissue source and belonged to the same species. We have found over the last ten years that the humeral cartilage is nearly identical for all the animals.) The elastic modulus increases exponentially through 80% tissue depth in both fresh and cryopreserved tissue; GAG concentration increases more linearly in fresh

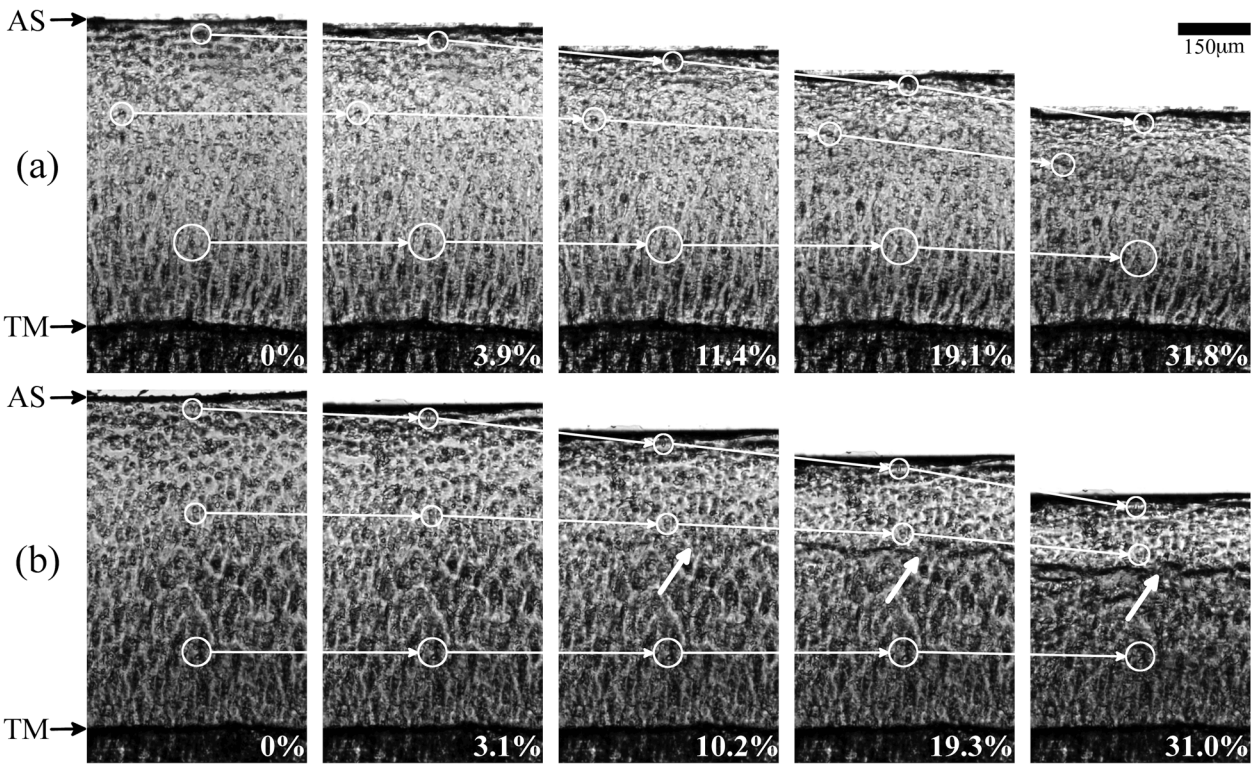

Fig. 2 Representative images used in the calculation of chondrocyte displacement and elastic modulus for (*a*) fresh tissue and (*b*) cryopreserved tissue. AS indicates the articular surface and TM indicates the tidemark. The white circles connected by arrows show the displacements of chondrocytes through several strains (%). The thick white arrows indicate the formation of a black line.

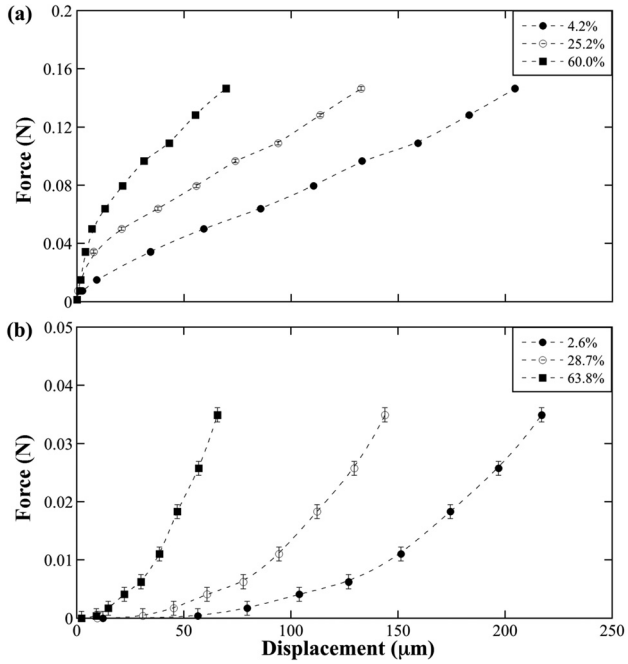

Fig. 3 Chondrocyte force–displacement curves for (*a*) fresh and (*b*) cryopreserved tissue at several relative depths (%). Each curve is illustrative of one chondrocyte from one sample tracked through consecutive images. *Y*-axis scales differ due to the significant reduction of cryopreserved tissue stiffness. Error bars include load sensor error, multimeter error, and force fluctuations at equilibrium.

tissue but exponentially in cryopreserved tissue. Cryopreserved GAG concentration is also markedly lower than fresh, especially in the SZ and TZ, and remains nearly constant before abruptly increasing at approximately 50% tissue depth. The numerical difference of fresh and cryopreserved tissue modulus also rises exponentially (data not shown). Cryopreserved tissue samples without Gd application had the same modulus profiles (data not shown).

Statistics. Statistically significant ($p < 0.05$) difference between fresh and cryopreserved cartilage moduli and GAG concentration were found for all same-depth ranges. There was high statistical difference ($p < 0.001$) between fresh and cryopreserved cartilage moduli for 0–10%, 20–30%, 30–40%, and 50–60% same-depth ranges. There was high statistical difference ($p < 0.001$) between fresh and cryopreserved cartilage GAG concentration for all same-depth ranges.

Discussion

Osteochondral grafting has great prospects in joint repair when using a properly functioning, long lasting implant. In addition to the depth-dependent elastic modulus of articular cartilage that is important for determining osteochondral graft viability, chondrocyte metabolism is at least in part controlled by mechanical stimulation through deformation of the cartilage extracellular matrix (ECM) [16]. Since articular cartilage is highly anisotropic, it is important to understand the depth-dependent biomechanical properties. These biomechanical properties are altered in cryopreserved osteochondral grafts, which can lead to reduced graft function and longevity. This study has provided clear indicators of cryodamage on biomechanical functionality, such as black line formation (Fig. 2), significantly altered force–displacement profiles (Fig. 3), and dramatically decreased depth-dependent elastic

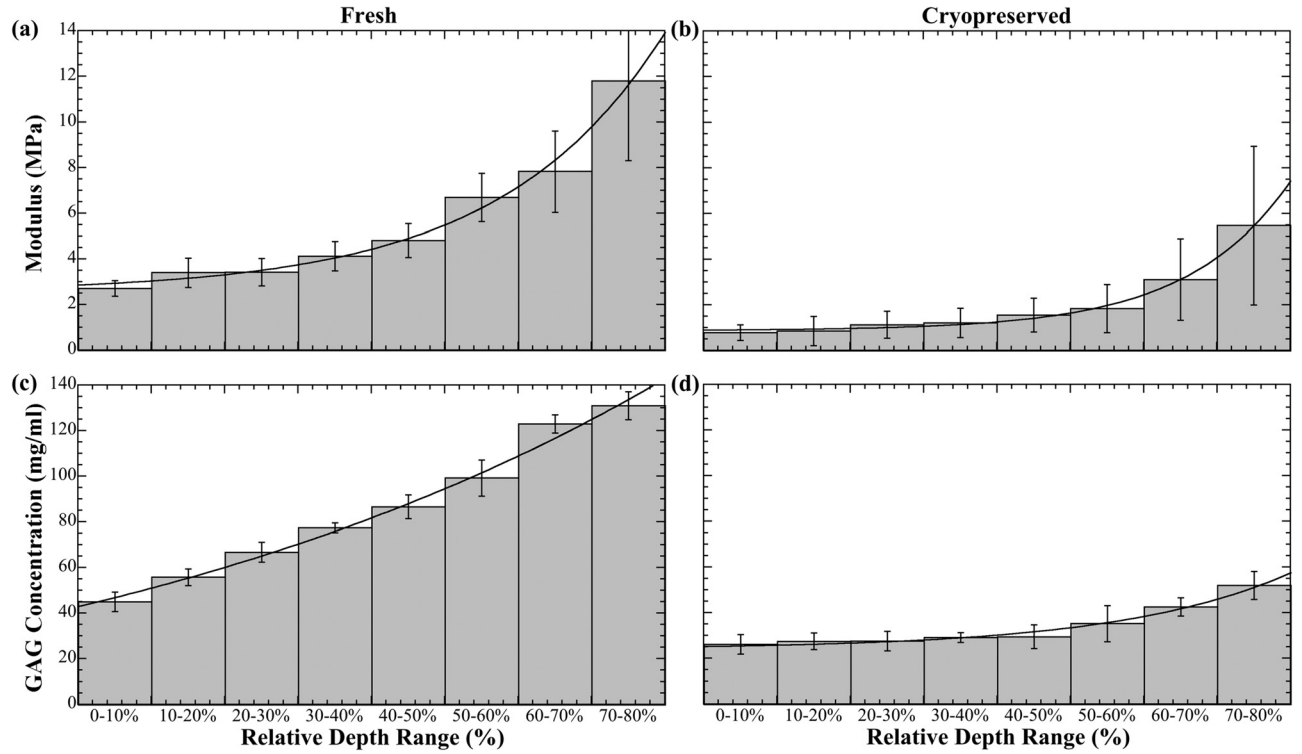

Fig. 4 Depth-dependent profiles of elastic modulus and GAG concentration. Depth is plotted on a relative scale where 0–10% indicates the SZ and all other percentage ranges indicate relative intratissue depth. Values and error bars are mean ± S.D. and modulus is fit exponentially through 80% relative depth as (*a*) $E_f = 2.57 + 0.25e^{0.45x}$ and (*b*) $E_c = 0.90 + 0.02e^{0.71x}$, where *x* is relative depth, and E_f and E_c are the elastic modulus of fresh and cryopreserved cartilage, respectively.

modulus (Fig. 4) giving rise to concerns about cryopreserved graft viability.

Visual Observations. The abrupt GAG concentration [4] increase at approximately 50% tissue depth explains the formation of the black line in the last three images of Fig. 2(*b*). Compared to the more linearly increasing GAG concentration [4] in fresh tissue that generates continuously increasing stiffness, the abrupt increase in degraded tissue creates a semirigid barrier forcing collagen fibers to bend sharply. A similar black line formation has also been observed in other degraded tissue experiments using μMRI [17–19].

Force–Displacement. Figure 3 has substantial implications for cryopreserved osteochondral implants. The concave-up and concave-down trends indicate a "toe-region" typically seen in the beginning of compression is not seen in fresh tissue, which may be a result of the incremental step resolution; i.e., step increments were approximately 30 μm, where much smaller increments may be needed to observe a toe-region. In contrast, a highly elongated toe-region is observed in cryopreserved tissue. Two explanations for this incident are: (1) depth-dependent changes in GAG concentration [4] postcryopreservation (Fig. 4) and (2) friction between the compression platen and cassette.

Modulus and GAG. First, a steadily increasing modulus (Fig. 4(*a*)) and nearly linearly increasing depth-dependent GAG concentration [4] (Fig. 4(*c*)) in fresh tissue produces smooth, continuous depth-dependent compression response when deformation originates at the AS. In cryopreserved tissue, a far more gradually increasing modulus (Fig. 4(*b*)) and GAG concentration [4] (Fig. 4(*d*)) in the upper zones (less than approximately 50% relative depth) indicates greatest compressive strain occurs almost simultaneously throughout a large depth range. The increasing modulus difference (data not shown) shows the depth-dependent exponential growth is slower in cryopreserved cartilage, also indicating compliance occurs through a large depth range. Therefore, as compression occurs at the AS, there is significantly less resistance contributed by successive depths. The simultaneous compression proceeds until maximum zonal compression is reached or includes deeper, stiffer regions. A cryopreserved osteochondral graft exhibiting this force–displacement trend could indicate improper depth-dependent functionality that may lead to insufficient axial load distributions, increased wear in the upper zones, and an overall increased wear rate.

Second, although care was taken to eliminate friction between the compression platen and cassette, a small amount of friction may have been present that could cause force readings not associated with the tissue. To the best of our abilities, experimental protocol was kept constant for all groups but an inadvertent inconsistency may have developed since experiments were performed over an extended period.

Depth-dependent elastic modulus measurements (Fig. 4) are made to only 80% relative depth, since chondrocyte displacements at greater depths are too small for accurate measurement at 4× objective magnification. This means bulk-tissue strains need to greatly exceed 35% to produce measurable intratissue strains at depths greater than 80%, which are uncharacteristic of physiological loading conditions. Also, the exponential cannot accurately predict the modulus at the TM due to the rapid divergence of the modulus at the cartilage–bone interface but describes the tissue well through 80% relative depth. The markedly reduced depth-dependent modulus in cryopreserved tissue suggests an inability for bearing heavy load such as the human body. Exponential growth of fresh and cryopreserved depth-dependent modulus difference (data not shown) suggests increased cryodamage effect with increased depth. These postcryopreservation depth-dependent abnormalities may lead to recurring osteoarthritic conditions and joint pain.

Correlations. There is a correlation of our depth-dependent findings and several other tissue studies of chondrocyte metabolism [20], osteochondral graft GAG production [21], and chondrocyte annihilation [14,15]. Other investigations found mechanical loading plays a crucial role in cartilage health by mechanically stimulating chondrocyte metabolic activity [20] for proteoglycan and GAG synthesis [22–24]. Since ECM deformation significantly affects chondrocyte shape and volume [20], altered depth-dependent tissue dynamics may lead to chondrocyte loading uncharacteristic of healthy cartilage. Then, cryopreserved cartilage may not possess the mechanical qualities required to stimulate chondrocyte metabolism for cartilage maintenance and regeneration, but higher magnification imaging is needed to verify abnormal volume deformation.

Frenkel et al. found that in several types of osteochondral grafts there was increased GAG loss with time after implantation and suggests reduced loading at the graft site (femoral trochlear groove) as one explanation [21]. They speculate hyalinelike cartilage produced by graft chondrocytes would quickly deteriorate from inability of grafts to withstand compressive forces, thereby limiting long-term proteoglycan synthesis. Although loading is less in this region, our investigation provides an additional explanation such that the reduced elastic modulus of cryopreserved grafts may decrease or eliminate chondrocyte metabolic activity.

Muldrew et al. found 1 yr after transplanting cryopreserved osteochondral grafts, chondrocytes were nonexistent in the intermediate zone (approximately 50% relative tissue depth) [14,15]. One possible explanation for this finding is the odd loading conditions in this zone, described as the black line at approximately the same depth (Fig. 2(*b*)). If loading of cryopreserved osteochondral grafts caused excessive collagen fiber bending, chondrocytes could be eradicated in that region.

Assumptions and Limitations. Our testing apparatus provides a novel technique for studying the depth-dependent biomechanical properties of articular cartilage. Using this experimental design, we are able to visually track the displacement of chondrocytes within the tissue through simple optical imaging, providing an additional method for biomechanical testing. Although our technique reduces the need for histological alteration, it forces us to utilize a confined–unconfined configuration since the in-plane image field of view allows for tissue expansion (unconfined), while the tissue is bound by the glass cassette (confined) in the optical path direction.

The added mass of the glass cassette, although minimal, could introduce other variables such as friction between the cassette and the clear glass window. We eliminated this effect by performing a multistep stress relaxation test. By finding the slope of the force–displacement curve, all other constant forces (e.g., friction) are ignored and only the tissue forces remain.

A limitation of this study is the use of only one cryopreservation method since several methods exist. In the future, it would be beneficial to test the depth-dependent mechanical functionality of articular cartilage using several cryopreservation techniques. Another limitation is the sample size of the groups. In order to strengthen the statistical comparison between groups, many additional samples are required.

Conclusion

This preliminary study has shown the effects of cryopreservation on the depth-dependent biomechanical function of canine humeral articular cartilage. The depth-dependent elastic modulus of cryopreserved cartilage was greatly reduced, and it is clear that cryopreservation causes damage to the tissue ECM. Our findings, when compared with other investigations, suggest the reduced depth-dependent modulus and improper intratissue loading of cryopreserved osteochondral grafts leads to increased wear, poor functionality, reduced chondrocyte metabolism, and poor long-term viability. In order to develop a proper storage method,

continued depth-dependent investigations of cryopreservation effects using additional cryopreservation techniques are of great importance.

Acknowledgment

Yang Xia is grateful to the National Institutes of Health for the R01 Grant (AR 052353). The authors thank Dr. Hani Sabbah (Henry Ford Hospital, Detroit) for providing the specimens, Ms. Janelle Spann (Michigan Resonance Imaging, Rochester Hills, MI) for providing the contrast agent, and Mr. Daniel Mittelstaedt (Oakland University, Rochester, MI), Mrs. Ji Hyun Lee (Oakland University, Rochester, MI), and Mr. Farid Badar (Oakland University, Rochester, MI) for editing.

References

[1] Maroudas, A., 1975, "Biophysical Chemistry of Cartilaginous Tissues With Special Reference to Solute and Fluid Transport," Biorheology, **12**(3–4), pp. 233–248.
[2] Venn, M., and Maroudas, A., 1977, "Chemical Composition and Swelling of Normal and Osteoarthrotic Femoral Head Cartilage. I. Chemical Composition," Ann. Rheum. Dis., **36**(2), pp. 121–129.
[3] Xia, Y., Zheng, S., and Bidthanapally, A., 2008, "Depth-Dependent Profiles of Glycosaminoglycans in Articular Cartilage by MicroMRI and Histochemistry," J. Magn. Reson. Imaging, **28**(1), pp. 151–157.
[4] Zheng, S., Xia, Y., Bidthanapally, A., Badar, F., Ilsar, I., and Duvoisin, N., 2009, "Damages to the Extracellular Matrix in Articular Cartilage due to Cryopreservation by Microscopic Magnetic Resonance Imaging and Biochemistry," Magn. Reson. Imaging, **27**(5), pp. 648–655.
[5] Chen, S. S., Falcovitz, Y. H., Schneiderman, R., Maroudas, A., and Sah, R. L., 2001, "Depth-Dependent Compressive Properties of Normal Aged Human Femoral Head Articular Cartilage: Relationship to Fixed Charge Density," Osteoarthritis Cartilage, **9**(6), pp. 561–569.
[6] Klein, T. J., Chaudhry, M., Bae, W. C., and Sah, R. L., 2007, "Depth-Dependent Biomechanical and Biochemical Properties of Fetal, Newborn, and Tissue-Engineered Articular Cartilage," J. Biomech., **40**(1), pp. 182–190.
[7] Laasanen, M. S., Toyras, J., Korhonen, R. K., Rieppo, J., Saarakkala, S., Nieminen, M. T., Hirvonen, J., and Jurvelin, J. S., 2003, "Biomechanical Properties of Knee Articular Cartilage," Biorheology, **40**(1–3), pp. 133–140.
[8] Szarko, M., and Xia, Y., 2012, "Direct Visualisation of the Depth-Dependent Mechanical Properties of Full-Thickness Articular Cartilage," Open J. Orthop., **2**, pp. 34–39.
[9] Donnan, F., 1924, "The Theory of Membrane Equilibria," Chem. Rev., **1**(1), pp. 72–90.
[10] Lai, W. M., Hou, J. S., and Mow, V. C., 1991, "A Triphasic Theory for the Swelling and Deformation Behaviors of Articular Cartilage," ASME J. Biomech. Eng., **113**(3), pp. 245–258.
[11] Maroudas, A., 1968, "Physicochemical Properties of Cartilage in the Light of Ion Exchange Theory," Biophys. J., **8**(5), pp. 575–595.
[12] Jomha, N. M., Lavoie, G., Muldrew, K., Schachar, N. S., and McGann, L. E., 2002, "Cryopreservation of Intact Human Articular Cartilage," J. Orthop. Res., **20**(6), pp. 1253–1255.
[13] Laouar, L., Fishbein, K., McGann, L. E., Horton, W. E., Spencer, R. G., and Jomha, N. M., 2007, "Cryopreservation of Porcine Articular Cartilage: MRI and Biochemical Results After Different Freezing Protocols," Cryobiology, **54**(1), pp. 36–43.
[14] Muldrew, K., Novak, K., Hurtig, M., Schachar, N., and McGann, L., 1993, "Cryopreservation of Articular Cartilage Using In Vitro and In Vivo Assays," Trans. Orthop. Res. Soc., **18**, p. 275.
[15] Muldrew, K., Novak, K., Yang, H., Zernicke, R., Schachar, N. S., and McGann, L. E., 2000, "Cryobiology of Articular Cartilage: Ice Morphology and Recovery of Chondrocytes," Cryobiology, **40**(2), pp. 102–109.
[16] Guilak, F., Sah, R., and Setton, L., 1997, "Physical Regulation of Cartilage Metabolism," *Basic Orthopaedic Biomechanics*, V. Mow, and W. Hayes, eds., Lippincott-Raven, Philadelphia, pp. 179–207.
[17] Wang, N., Kahn, D., Badar, F., and Xia, Y., 2014, "Molecular Origin of a Loading-Induced Black Layer in the Deep Region of Articular Cartilage at the Magic Angle," J. Magn. Reson. Imaging (in press).
[18] Alhadlaq, H. A., and Xia, Y., 2004, "The Structural Adaptations in Compressed Articular Cartilage by Microscopic MRI (microMRI) T(2) Anisotropy," Osteoarthritis Cartilage, **12**(11), pp. 887–894.
[19] Alhadlaq, H. A., and Xia, Y., 2005, "Modifications of Orientational Dependence of Microscopic Magnetic Resonance Imaging T2 Anisotropy in Compressed Articular Cartilage," J. Magn. Reson. Imaging, **22**(5), pp. 665–673.
[20] Guilak, F., Jones, W. R., Ting-Beall, H. P., and Lee, G. M., 1999, "The Deformation Behavior and Mechanical Properties of Chondrocytes in Articular Cartilage," Osteoarthritis Cartilage, **7**(1), pp. 59–70.
[21] Frenkel, S. R., Kubiak, E. N., and Truncale, K. G., 2006, "The Repair Response to Osteochondral Implant Types in a Rabbit Model," Cell Tissue Banking, **7**(1), pp. 29–37.
[22] Brittberg, M., Lindahl, A., Nilsson, A., Ohlsson, C., Isaksson, O., and Peterson, L., 1994, "Treatment of Deep Cartilage Defects in the Knee With Autologous Chondrocyte Transplantation," N. Engl. J. Med., **331**(14), pp. 889–895.
[23] Gole, M. D., Poulsen, D., Marzo, J. M., Ko, S. H., and Ziv, I., 2004, "Chondrocyte Viability in Press-Fit Cryopreserved Osteochondral Allografts," J. Orthop. Res., **22**(4), pp. 781–787.
[24] Shieh, A. C., and Athanasiou, K. A., 2003, "Principles of Cell Mechanics for Cartilage Tissue Engineering," Ann. Biomed. Eng., **31**(1), pp. 1–11.